FISEVIER

Contents lists available at ScienceDirect

Infrared Physics & Technology

journal homepage: www.elsevier.com/locate/infrared



Regular article

Low-frequency noise properties of *p*-type GaAs/AlGaAs heterojunction detectors



Seyoum Wolde^a, Y.F. Lao^a, P.K.D.D.P. Pitigala^a, A.G.U. Perera^{a,*}, L.H. Li^b, S.P. Khanna^{b,1}, E.H. Linfield^b

- ^a Department of Physics and Astronomy, Georgia State University, Atlanta, GA 30303, USA
- ^b The School of Electronic and Electrical Engineering, University of Leeds, Leeds LS2 9JT, UK

HIGHLIGHTS

- At low temperature and low bias, the G-R type shot noise masks all other noise components.
- Grading the barrier of GaAs/AlGaAs heterostructures enhances the escape probability of carriers.
- Detectivity can be improved by optimizing emitter thickness and increasing escape probability.

ARTICLE INFO

Article history: Received 1 July 2016 Revised 20 July 2016 Accepted 21 July 2016 Available online 22 July 2016

Keywords: Graded barrier Noise AlGaAs GaAs Gain

ABSTRACT

We have measured and analyzed, at different temperatures and bias voltages, the dark noise spectra of GaAs/AlGaAs heterojunction infrared photodetectors, where a highly doped GaAs emitter is sandwiched between two AlGaAs barriers. The noise and gain mechanisms associated with the carrier transport are investigated, and it is shown that a lower noise spectral density is observed for a device with a flat barrier, and thicker emitter. Despite the lower noise power spectral density of flat barrier device, comparison of the dark and photocurrent noise gain between flat and graded barrier samples confirmed that the escape probability of carriers (or detectivity) is enhanced by grading the barrier. The grading suppresses recombination owing to the higher momentum of carriers in the barrier. Optimizing the emitter thickness of the graded barrier to enhance the absorption efficiency, and increase the escape probability and lower the dark current, enhances the specific detectivity of devices.

© 2016 Elsevier B.V. All rights reserved.

1. Introduction

Understanding the physical origins and mechanisms responsible for different types of electronic noise is important in optimizing the performance of a broad range of electronic devices. Electronic noise can originate from dark currents, temperature fluctuations, and trap states. The fundamental noise components (shot noise and thermal noise), are frequency independent, and can be controlled to some extent by the choice of device architecture, and through optimizing the detailed design [1], including the choice of active materials, growth technique, operating temperature, and doping levels.

The presence of defects and impurities results in large fluctuations in electronic conductivity through fluctuations of carrier density [2], mobility [3] or a combination of the two [4–6]. The net

charge of any defect is then determined by the emission and capture of carriers. A defect trap is charged upon carrier emission, and neutralized upon carrier capture. These fluctuations in carrier numbers due to trapping, and in some cases phonon scattering, lead to generation-recombination (G-R) noise. Studies of hole traps in unintentionally *p*-type doped GaAs layers have been investigated previously [7], together with the low-frequency noise properties of beryllium-doped GaAs/AlAs [1] quantum well and epitaxial layers of Al_{0.5}Ga_{0.5}As [8] grown by molecular beam epitaxy (MBE).

In this article, we investigate *p*-type beryllium-doped infrared photodetectors in which a GaAs emitter is sandwiched between undoped AlGaAs barriers. Having a doped emitter can lead to excess noise owing to traps formed by ionized clustering of impurities [9], and this can reduce the gain of optoelectronic devices. This G-R noise has the general property that the noise spectral density increases at lower frequencies and so low-frequency noise (LFN) measurement can be utilized as a diagnostic tool to characterize devices [10]. The aim of our present study is to characterize the various contributions of noise on the performance of an infrared photodetector, and specifically their effect on device gain. We

^{*} Corresponding author.

E-mail address: uperera@phy-astr.gsu.edu (A.G.U. Perera).

¹ Current address: Physics of Energy Harvesting, CSIR-National Physical Laboratory, New Delhi, India.

investigate the noise and gain mechanisms associated with carrier transport for different barriers and emitter thicknesses in terms of a range of parameters used for optimizing the detectivity of devices, including the dark current, photo-absorption, and capture probability.

2. Device structures and experimental procedures

Four detector designs were investigated (Table 1), with the valence band profile of the structures being shown in Fig. 1. All structures have a highly p-doped $(1 \times 10^{19} \text{ cm}^{-3})$ emitter sandwiched between two undoped AlGaAs barriers. In three of the structures, one of the barriers is graded, whilst in the fourth structure, both barriers have a constant height. The width of the graded barrier is 80 nm in SP1005, SP1006 and SP1007, and the aluminum mole fraction is changed uniformly from 0.45 (X_1) to 0.75 (X_2) by adjusting the cell temperatures during growth to give a "continuous" (also known as "averaging") approach to the grading. The side of the barrier with the lower aluminum mole fraction (X_1) is next to the bottom contact. A second barrier with a constant 0.57 (X_3) aluminum mole fraction then separates the emitter from the top contact, and has a width of 400 nm. SP1005, SP1006, and SP1007 differ from each other by the emitter thickness. In SP1001, both barriers have a constant height: the first barrier has a mole fraction of 0.75 ($X_1 = X_2$), and the second barrier 0.57 (X_3). For all devices, photo-absorption in the emitter excites carriers from the light/ heavy hole bands into the split-off band. The excited carriers then escape from the emitter layer after scattering out of split-off band back into the light/heavy hole band at the emitter-barrier interface [11] as shown in Fig. 1. Detailed explanations of detection mechanism, as well as details of the growth of all structures, have been reported previously in Pitigala et al. [11,12].

In order to determine the low frequency noise, devices were biased with a DC voltage source. The voltage and current noise

Table 1 Device structure details listing the different aluminum mole fractions $(X_1, X_2, \text{ and } X_3)$ used for the barriers, as illustrated in Fig. 1. All emitters are p-doped at 1×10^{19} cm⁻³.

Device no.	Lower edge (X_1)	Higher edge (X_2)	Constant barrier (X_3)	Emitter thickness (W) (nm)
SP1001	0.75	0.75	0.57	80
SP1005	0.45	0.75	0.57	20
SP1006	0.45	0.75	0.57	50
SP1007	0.45	0.75	0.57	80

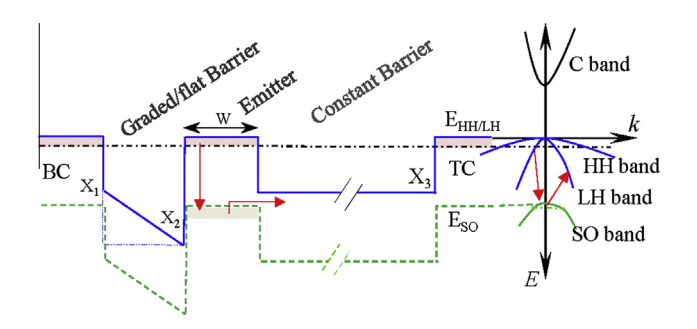


Fig. 1. Schematic diagram of the valence band structure at wave vector k=0 and E-k diagram for an emitter region of the device: for the graded barrier structures $X_1 < X_2$ and in the constant barrier structure $X_1 = X_2$. The emitter thicknesses (W) and Al mole fractions (X_i) are tabulated in **Table 1**. The top contact (TC), bottom contact (BC), and the emitter are p-doped ($10^{19} \, \mathrm{cm}^{-3}$). The dashed-dotted line represents the fermi level of heavy hole (HH)/light hole (LH) band. The dotted line represents split-off (SO) band in the device. The arrows indicate the possible transition mechanisms: a direct transition from LH to SO band followed by scattering back to LH band.

spectra were then amplified using a Stanford Research System SR560 low-noise voltage amplifier with a fixed gain of G = 1000and an SR 570 low-noise current preamplifier, respectively, and measured using an HP SRS-SR785 spectrum analyzer in a frequency range of 1 Hz-102 kHz. Devices were mounted on a holder placed on the cold head of a liquid nitrogen-cooled dewar, and the temperature was measured using a 330 Lake Shore controller. The detector, amplifier, and dry battery providing the bias voltage were shielded in a grounded aluminum box to prevent the external environment influencing the background noise. The input voltage noise of the apparatus was determined by shorting out the sample; and was found to be independent of temperature. The noise power spectral density was then measured in three to four different overlapping frequency spans. At low frequencies, the small bin width of 0.125 Hz is used to ensure better frequency resolution and accuracy of the measurements.

3. Results and discussion

The four most common noise components are thermal, shot, G-R, and 1/f. Thermal noise is due to thermal motion of carriers and is given by $S_{th} = 4KT/R$, where T is the temperature and R is the resistance of the device, and this noise mechanism is frequency independent. Shot noise is also frequency independent, and originates from the discrete nature of carriers; its power spectral density is given by $S_{sh} = 2eI$, where I is the current supplied by the DC source. Defects, impurities, and band discontinuities can, however, trap carriers, interrupting the current flow. If the trap levels are all identical, then there is a continuous emission and capture of holes between the traps and the valence band. Hence, the number of trapped and free carriers will fluctuate with the generation-recombination spectrum of the carriers due to these fluctuations being given by [13,14]:

$$S_n(f) = \langle (\Delta n)^2 \rangle \frac{4\tau}{1 + (2\pi f \tau)^2},\tag{1}$$

where $\langle (\Delta n)^2 \rangle$ is the variance of the number of trapped carriers, f is frequency and τ is the characteristic time. At a given temperature, the maximum G-R noise level is observed when $2\pi f \tau = 1$. Superposition of many G-R processes with a smooth distribution of characteristic times then leads to a 1/f noise spectrum [1], where the intensity is proportional to the number of trap centers.

The origin of 1/f noise is generally explained by two models: noise related to mobility fluctuations $(\Delta\mu)$, and noise related to carrier density fluctuations (ΔN) . However, the conductance, or resistance R, of a semiconductor also fluctuates with a 1/f spectrum [13]. The conductance fluctuations of an ohmic sample can be measured as voltage fluctuations when a constant current I is passed through the sample, or as current fluctuations when the voltage drop V across the sample is kept constant. The low-frequency 1/f noise behavior is expressed simply by the equation [13]:

$$\frac{S_R(f)}{R^2} = \frac{S_I(f)}{I^2} = \frac{S_V(f)}{V^2} = \frac{A_{1/f}}{f},\tag{2}$$

where $A_{1/f}$ is a measure of the relative amplitude of the noise of the sample, and $S_R(f), S_V(f)$, and $S_I(f)$ are the noise power spectral densities of resistance, voltage, and current, respectively. The G-R noise (Eq. (1)) may be associated with multiple trap levels of different relaxation times τ_i , which are assumed to be uncorrelated, and hence the corresponding terms can be added. The total noise power spectral density is a combination of 1/f noise, G-R noise, thermal noise, and shot noise, and can be described by the equation [13]:

$$S(f,T) = \frac{A(T)I^{2}}{f^{\alpha}} + \sum_{i=1}^{n} \frac{B(T)\tau_{i}}{1 + (2\pi f \tau_{i})^{2}} + S_{white}$$
(3)

Download English Version:

https://daneshyari.com/en/article/1783895

Download Persian Version:

https://daneshyari.com/article/1783895

<u>Daneshyari.com</u>